eFood

WILEY

eFood

RESEARCH ARTICLE OPEN ACCESS

Anti-Inflammatory and Antioxidant Activities of Polyphenols From Loquat (*Eriobotrya japonica* Lindl.) Leaf Hair in Lipopolysaccharide-Induced In Vitro and In Vivo Models

Can Hu[1] | Jiazheng Hu[2] | Hongyu Ye[2] | Mengxin Wang[2] | Manxi Wu[2] | Han Yang[2] | Kang Chen[4] | Jinping Cao[2] | Yanshuai Wang[3] | Yue Wang[2,5,6,7] | Chongde Sun[2]

[1]Stomatology Hospital, School of Stomatology, Zhejiang University School of Medicine, Hangzhou, China | [2]Fruit Science Institute, College of Agriculture and Biotechnology, Zhejiang University, Hangzhou, China | [3]Department of Hepatobiliary and Pancreatic Surgery, The First Affiliated Hospital, School of Medicine, Zhejiang University, Hangzhou, China | [4]Liandu Agriculture and Rural Bureau, Lishui, China | [5]Center for Balance Architecture, Zhejiang University, Hangzhou, China | [6]The Rural Development Academy, Zhejiang University, Hangzhou, China | [7]The Architectural Design & Research Institute of Zhejiang University Co. Ltd., Hangzhou, China

Correspondence: Yanshuai Wang (wyshc@zju.edu.cn) | Yue Wang (fruit@zju.edu.cn)

Received: 18 March 2025 | **Revised:** 5 May 2025 | **Accepted:** 12 May 2025

Funding: This article was supported by the Fundamental Research Funds for the Zhejiang Provincial Universities (226-2024-00211).

Keywords: anti-inflammation | antioxidant | Jak2–Stat3 pathway | loquat leaf hair | polyphenols

ABSTRACT

This study aimed to characterize polyphenols present in Loquat (*Eriobotrya japonica* Lindl.) leaf hair (LLH) and evaluate their antioxidant and anti-inflammatory effects in lipopolysaccharide (LPS)-induced inflammation models In Vitro and In Vivo. Ultra-performance liquid chromatography coupled with UPLC-HRMS identified 24 compounds in LLH, including 21 polyphenols, notably revealing the presence of four polymethoxyflavones previously unreported in loquat. Antioxidant evaluations (ABTS, DPPH, FRAP, and ORAC) confirmed robust radical-scavenging and reducing capabilities of LLH extract. In Vitro studies utilizing human liver L02 cells demonstrated that LLH significantly suppressed LPS-induced reactive oxygen species (ROS) generation, preserved antioxidant enzyme activities (CAT, SOD, and GSH-Px), and upregulated antioxidant-related genes (*Nrf2*, *Cat*, *Sod1*, and *Gpx1*). Furthermore, LLH pretreatment markedly inhibited LPS-induced nitric oxide (NO) release, inflammatory cytokine (IL-1β, IL-6, and TNF-α) production, and downregulated the Jak2–Stat3 inflammatory signaling pathway. Consistently, In Vivo experiments using an LPS-induced acute liver injury mouse model revealed that oral administration of LLH significantly reduced hepatic oxidative stress and inflammation by restoring antioxidant enzyme activities, enhancing *Nrf2*-mediated antioxidant pathways, and suppressing inflammatory mediators and Jak2–Stat3 signaling in liver. Collectively, these findings demonstrate LLH polyphenols' potent antioxidant and anti-inflammatory effects and suggest their potential as natural functional agents for managing inflammation-related oxidative stress.

1 | Introduction

Loquat is a plant of the genus *Eriobotrya* in the family Rosaceae, which is not only fresh fruit, but its leaves are used as medicine and food homologous products due to their antioxidant, anti-inflammation, and organ function-regulating properties. The biological activities of loquat are directly linked to its rich phytochemical composition. Previous studies have shown that

This is an open access article under the terms of the Creative Commons Attribution License, which permits use, distribution and reproduction in any medium, provided the original work is properly cited.

© 2025 The Author(s). *eFood* published by John Wiley & Sons Australia, Ltd. on behalf of International Association of Dietetic Nutrition and Safety.

loquat leaves contain active substances such as chlorogenic acid (Xu et al. 2014), ursolic acid (Tan et al. 2019), and oleanolic acid (B. Chen et al. 2017), which may be the main components responsible for its anti-inflammatory effects. However, the leaf hair composition of loquat leaves has not been reported and there is a large body of literature suggesting that the glandular and nonglandular hair tissues of the plant may be sites of natural product enrichment (Y. Liu et al. 2019; Santos Tozin et al. 2016). Therefore, the bioactive substances and their effects found in the dense trichomes covering the back of the loquat leaves have piqued our research interest.

Anti-inflammatory is the main bioactive effect of loquat. Due to tissue damage, viruses, immune factors and other stimuli, the body induces the aggregation of immune cells (Ratanji et al. 2014), the release of cytokines (Fajgenbaum and June 2020), and the production of inflammatory mediators (Thanou et al. 2021), resulting in localized redness, swelling, heat pain, or systemic fever, fatigue, anorexia, and other inflammatory response symptoms (Lei et al. 2015). Chronic inflammatory responses may lead to damage such as tumors (Grivennikov and Karin 2011) and autoimmune imbalances (Thanou et al. 2021). Therefore, inhibition of early inflammation is an important means of health care and medical treatment. Lipopolysaccharide (LPS), as a common inflammatory inducer, can be leaked from the intestine to other tissues, such as the liver, under the mediation of various factors, further exacerbating the burden on the liver (P. Zhang et al. 2022; Zheng and Wang 2021) Loquat, as a traditional medicinal and food source with anti-inflammatory properties, has been mainly studied for its ability of leaf mesophyll, but there are relatively few reports on its bioactivities of leaf hair. Therefore, we aim to use natural products from loquat as materials to study its inhibition of LPS-induced liver inflammation and conduct preliminary mechanistic investigations.

Oxidative stress often accompanies inflammation and is a critical factor in LPS-induced tissue damage (Qiu et al. 2025). Excessive production of reactive oxygen species (ROS) during an inflammatory response can directly injure cellular components and further amplify pro-inflammatory signaling. Polyphenols, a major class of phytochemicals in many medicinal plants (including loquat), are well known for their potent antioxidant activities. They can directly scavenge ROS due to their phenolic hydroxyl groups and conjugated structures (Li et al. 2023), thereby protecting cells from oxidative damage. Additionally, polyphenols activate endogenous antioxidant defenses by modulating redox-sensitive pathways such as the nuclear factor erythroid 2-related factor 2 (Nrf2)/Keap1 system (Yin et al. 2024). Activation of the Nrf2–Keap1 pathway upregulates numerous antioxidant and phase II detoxification enzymes (e.g., heme oxygenase-1 (HO-1), superoxide dismutase (SOD), and glutathione peroxidase (GSH-Px)) (Y. Chen et al. 2024). Through these mechanisms—scavenging ROS and boosting enzymatic antioxidants—polyphenols help maintain redox homeostasis and mitigate oxidative stress-related tissue damage (Wang et al. 2022).

In this study, UPLC–HRMS was used to identify the polyphenolic constituents of loquat leaf hairs (LLH), and we evaluated the extract's anti-inflammatory and antioxidant effects against LPS-induced injury in both cell and mouse models. Further mechanistic investigations were carried out to elucidate the pathways involved in these effects. In particular, we examined the modulation of the Janus kinase 2 (Jak2)–signal transducer and activator of transcription 3 (Stat3) signaling pathway and the Nrf2–Keap1 pathway by LLH treatment. To our knowledge, this is the first study to characterize the active compounds in LLH and to demonstrate their combined anti-inflammatory and antioxidant activities, providing a basis for the development of medicinal and functional food products.

2 | Materials and Methods

2.1 | Materials and Chemicals

Loquat leaves of "luoyangqing" variety were harvested from Hangzhou, Zhejiang Province in August 2021. The intact loquat leaves of the current year without pests and diseases were taken off, washed with double-distilled water (ddH_2O), and dried at 20°C. The LLH were collected with a soft brush and frozen with liquid nitrogen, then stored at −80°C. Human normal liver cell line L02 was purchased from COBIOER Bioscience Co. Ltd. (Nanjing, China). Enzyme-Linked Immunosorbent Assay (ELISA) kits of IL-1β, IL-6, TNF-α, Jak2, and phospho-JAK2 (p-JAK2) were purchased from Abcam (Shanghai, China). Trizol reagent, ELISA kits of STAT3 and phospho-STAT3 (p-STAT3) were purchased from Invitrogen Company (Shanghai, China). RPMI-1640 medium, trypsin–EDTA were purchased from Gibco (Waltham, MA, USA). Cell-Counting Kit 8 was purchased from Dojindo (Shanghai, China). PrimeScript RT reagent kit with gDNA Eraser was purchased from Takara (Dalian, China). SsoFast EvaGreen Supermix was purchased from Bio-Rad (Hercules, CA, USA). Methanol, acetonitrile, formic acid of HPLC grade were purchased from Sigma-Aldrich (Shanghai, China). 2′,7′-Dichlorodihydrofluorescein diacetate (DCFH-DA) were purchased from Beyotime Biotechnology (Shanghai, China). 2,2-Diphenly-1-picrylhydrazyl (DPPH), methanol, 2,2′-azino-bis(3-ethylbenzothiazoline-6-sulfonic acid) (ABTS), potassium persulfate ($K_2S_2O_8$), sodium acetate, 2,4,6-tris(2-pyridyl)-s-triazine (TPTZ), ferric chloride, hydrochloric acid, acetic acid, Na_2HPO_4, NaH_2PO_4, 2,2′-azobis(2-methylpropionamidine) dihydrochloride (AAPH), sodium fluorescein, Trolox, and other reagents were of analytical grade purchased from Sinopharm Chemical Reagents Co. Ltd. (Shanghai, China). ddH_2O was used in all experiments. Samples injected in UPLC systems were filtered through a 0.22 μm membrane.

2.2 | UPLC and UPLC–MS Analysis of Loquat Leaf Hair

LLH were extracted using an optimized ultrasonic-assisted method to maximize polyphenol yield while minimizing thermal degradation. Briefly, 1.0 g of LLH powder was mixed with 10 mL of 90% ethanol (v/v). The solid–liquid ratio of 1:10 (g:mL) was optimized via single-factor experiments, balancing yield and solvent economy. Ultrasonic extraction was performed at 30°C for 60 min to avoid overheating-induced degradation of flavonoids and phenolic acids, with temperature monitored using a digital thermocouple. Following extraction, the mixture

was filtered through filter paper, and the supernatant was concentrated by rotary evaporation at 30°C under reduced pressure (80 RPM) to remove ethanol, minimizing oxidation of polyphenols. The residual aqueous phase was freeze-dried using a vacuum centrifugal system (30°C, 10 mbar) to obtain a dry extract.

The powder was dissolved in chromatographic methanol for substance detection. Ultrahigh-performance liquid chromatography (UPLC) and mass spectrometry were used for substance detection of the extract. The detection system was as follows.

2.2.1 | UPLC Detection System

ACQUITY UPLC HSS T3 (1.8 μm, 2.1 × 100 mm) as the stationary phase; the mobile phase consisted of water containing 1% formic acid (mobile Phase A) and acetonitrile containing 1% formic acid (mobile Phase B). The gradient elution procedure was: 0~20 min, 5%~95% B; 20~22 min, 95% B; 22~23 min, 95%~5% B; 23~25 min, 5% B. The scanning wavelength was set at 254 and 280 nm, the flow rate was 0.3 mL/min, the column temperature was 50°C, and the injection volume was 2 μL.

2.2.2 | Mass Detection System

An AB Triple TOF 5600^{plus} system (AB SCIEX, MA, USA) equipped with an electron spray ionization (ESI) source in negative mode was used for mass analysis. Scanning mode was positive and negative ion scanning range from 100 to 1500 m/z. The Ion Source Gas 1 (GS1) and Ion Source Gas 2 (GS2) was 55 psi. The Curtain Gas (CUR) was 35 psi. The ion source temperature (TEM) was 600°C for positive mode and 550°C for negative mode. The ion spray voltage (IS) was 5500 V (positive) and −4500 V (negative). In first-class scanning, the declustering potential (DP) was 100 V and the collision energy (CE) was 10 V. In secondary scanning: MASS spectrometry data were collected using TOF MS-Product Ion-IDA mode. The collision-induced dissociation (CID) was 40 ± 20 eV. Before sampling, the Calibrant Delivery System (CDS) was used for mass axis correction to make the mass axis error < 2 ppm.

2.3 | Cell Culture and NO Release Analysis

Human normal liver cell line L02 was cultured in a constant temperature and humidity incubator (37°C, 5% CO_2) using RPMI-1640 complete medium (containing 10% fetal bovine serum). Cells were passaged using trypsin–EDTA when they had grown to 80% confluency. The logarithmic growth phase cells were inoculated into 96-well plates at a density of 5×10^4 cells/well and incubated for 24 h, then replaced with fresh medium. The extracts of LLH at different concentrations (12.5 to 100 μg/mL) were dissolved in DMSO and then added into the medium (the final concentration of DMSO was lower than 0.1%). After incubation for 24 h, 0.1 μg/mL LPS was added to the culture medium for another 12 h. The concentrations of NO in the culture medium were determined according to the NO detection kit. DMSO was used as a solvent control and each treatment had three biological replicates.

2.4 | Cell Viability Assay

Cell viability was determined by CCK-8 assay. Cells in logarithmic growth phase were seeded in 96-well plates at a density of 5×10^4 cells/well, and after 24 h of incubation, fresh medium was replaced. LLH of different concentrations from 12.5 to 200 μg/mL were dissolved in DMSO and added to the medium (the final concentration of DMSO was lower than 0.5%), and the incubation was continued for 48 h. Then the complete medium was replaced with serum-free medium containing 10% CCK-8 reagent and incubated for 1 h. The absorbance values at 450 and 620 nm were measured with a microplate reader. DMSO was used as the solvent control and each treatment had three biological replicates.

2.5 | Chemical Antioxidant Capacity Assay

The free radical scavenging (ABTS, DPPH, ORAC) and iron ion reduction (FRAP) of LLH were evaluated using four chemical antioxidant methods. All assays were performed in triplicate at room temperature unless otherwise stated.

2.5.1 | ABTS Radical Scavenging Assay

ABTS working solution was prepared by mixing 50 mL of 7 mM ABTS with 50 mL of 2.6 mM potassium persulfate and allowing the reaction to proceed in the dark for 12 h at room temperature. The mixture was then diluted (~28-fold, $OD_{734} \approx 0.63$) before use. A 10 μL aliquot of the appropriately diluted sample was mixed with 200 μL of the ABTS working solution and incubated in the dark for 5 min. Absorbance at 734 nm was recorded using a microplate reader. Trolox was used as the standard, and results were expressed as mg Trolox/g FW.

2.5.2 | DPPH Radical Scavenging Assay

A 2 μL aliquot of the diluted sample was added to 198 μL of freshly prepared 60 μM DPPH solution and incubated for 2 h in the dark at room temperature. Absorbance at 517 nm was measured using a microplate reader. Trolox served as the standard, and results were expressed as mg Trolox/g FW.

2.5.3 | FRAP Assay (Ferric Reducing Antioxidant Power)

The FRAP working solution was prepared by mixing 100 mL of 300 mM sodium acetate buffer (pH 3.6), 10 mL of 10 mM TPTZ solution, and 10 mL of 20 mM ferric chloride. A 20 μL aliquot of the diluted sample was combined with 180 μL of the FRAP working solution and incubated for 5 min in the dark. Absorbance at 593 nm was measured using a microplate reader.

Trolox was used as the reference, and results were expressed as mg Trolox Equivalent (TE)/g FW.

2.5.4 | ORAC Assay (Oxygen Radical Absorbance Capacity)

A 25 μL aliquot of the diluted sample was mixed with 150 μL of 40 nM sodium fluorescein solution and incubated at 37°C in the dark for 10 min. Then, 25 μL of 750 mM AAPH solution was added, and fluorescence intensity was recorded every 2 min for 2 h (excitation: 485 nm, emission: 535 nm) using a microplate reader. Phosphate-buffered saline (PBS) served as a blank control, and wells without AAPH were used to determine the initial fluorescence intensity. The antioxidant capacity was calculated based on the area under the fluorescence decay curve (AUC), with Trolox as the reference. Results were expressed as mg TE/g FW.

2.6 | LPS Induced Oxidative Stress in L02 Cell Line and ROS Detection

Cells were first cultured in serum-free RPMI 1640 medium for 24 h. LLH extracts were prepared in DMSO to achieve a final concentration of 0.1% and then applied to the cells for 6 h. DMSO served as the solvent control. LPS was added at a final concentration of 0.1 μg/mL. For ROS detection, cells were rinsed twice with PBS before treatment with 10 μM DCFH-DA diluted in serum-free medium. After incubation at 37°C for 20 min, excess DCFH-DA was removed, and fluorescence intensity was measured using a microplate reader (excitation: 488 nm, emission: 525 nm). Each experiment was conducted in triplicate.

2.7 | Antioxidant Enzyme Activity Assay

The activities of antioxidant enzymes, including catalase (CAT), SOD, and glutathione peroxidase (GSH-Px), were determined using commercial assay kits from Nanjing Jiancheng Bio Co. (Nanjing, China). All procedures were performed following the manufacturer's protocols.

2.8 | Animal Assay

Male C57BL/6J mice (6-week-old, 20–22 g) were housed in sterile, ventilated cages (5 mice/cage) in an SPF facility at 22°C ± 2°C, 50% ± 5% relative humidity, and a 12:12 h light–dark cycle (lights on at 7:00 a.m.). Cages were enriched with autoclaved corn cob bedding, paper nesting material, and free access to sterile rodent chow (LabDiet 5K52, St. Louis, MO, USA) and reverse-osmosis water. Mice were acclimatized for 1 week before experiments. The mice were divided into 5 groups with 10 mice in each group, namely, control group (fed with water, intraperitoneal injection of normal saline), model group (fed with water, intraperitoneally injected with 0.25 mg/kg LPS for 7 days), low-dose group (25 mg/kg LLH by intragastric administration), medium-dose group (50 mg/kg LLH by intragastric administration), high-dose group (100 mg/kg LLH by intragastric administration). After continuous gavage for 21 d in the treatment group, 0.25 mg/kg LPS was intraperitoneally injected while maintaining the gavage for 7 d. After 28 days of treatment, mice were anesthetized with isoflurane (2%–3% in oxygen, 1 L/min) to induce mild sedation, followed by cervical dislocation performed by trained personnel. This humane euthanasia method was approved by the Zhejiang University Animal Experiment Center (Ethics Number: ZJU20210512) and adheres to GB/T 35892-2018 guidelines. Immediately post-euthanasia, livers were excised, rinsed in ice-cold PBS, blotted dry, and snap-frozen in liquid nitrogen for subsequent oxidative stress and inflammatory marker analyses.

2.9 | Quantitative Real-Time PCR Assay

L02 cells were seeded on 6-well plates at a density of 1×10^6 cells/well and incubated for 24 h. After replacing the medium, the extracts of LLH at different concentrations of 12.5, 25, and 100 μg/mL added into the medium. After incubation for 24 h, 0.1 μg/mL LPS was added and incubated for 12 h. Trizol reagent was used to extract total cellular RNA. For animal experiments, harvested livers were ground using a homogenizer, and total liver RNA was extracted. The complementary DNA (cDNA) was synthesized using the PrimeScript RT Reagent Kit with gDNA Eraser (Takara, RR047A). QRT-PCR was carried out in the CFX96 instrument (Bio-Rad) using the SsoFast EvaGreen Supermix Kit (BioRad, 1725202). The sequences of qRT-PCR primers are shown in Table 1, and β-actin was used as a control. Relative levels of gene expression were calculated using the comparison ($2^{-\Delta\Delta CT}$) method.

2.10 | Enzyme-Linked Immunosorbent Assay (ELISA) Assay

ELISA assays were performed using commercial kits according to the product instructions, with three replicates for each cell assay, and five biological replicates for animal assay.

2.11 | Statistics

Experimental results were presented as mean ± standard error of the mean (SEM). SPSS (version 19.0, IBM, Armonk, NY, USA) were used for data analyzing. GraphPad Prism (version 8.0, GraphPad Software Inc., San Diego, CA, USA) were used for data display. Statistical significance was determined by one-way analysis of variance (ANOVA) followed by Tukey's post hoc test. Values were considered significantly different at $p < 0.05$, and for multiple comparisons.

3 | Results

3.1 | Identification of Phenolic Components in Loquat Leaf Hair

UPLC–MS was used for identifying the compounds in LLH. As shown in Figure 1 and Table 2, a total of 24 compounds

TABLE 1 | Primers used in the real-time polymerase chain reaction (RT-PCR).

Source	Gene	Forward primer (5′ to 3′)	Reverse primer (3′ to 5′)
Human	*β-actin*	GTGGCCGAGGACTTTGATTG	AGTGGGGTGGCTTTTAGGATG
Human	*iNOS*	CAGGACCACACCCCCTAGGA	AGCCACATACCGAGCCATGC
Human	*IL-1β*	GTGTCCTGCGTGTTGAAAGAT	GAGTTGGGCATTGGTGTAGAC
Human	*IL-6*	ACCCCTGACCCAACCACAAAT	AGCTGCGCAGAATGAGATGAGTT
Human	*TNF-α*	CACAGTGAAGTGCTGGCAAC	GGCGATTACAGACACAACTCC
Human	*Jak2*	AGCCTATCGGCATGGAATATCT	TAACACTGCCATCCCAAGACA
Human	*Stat3*	ACCAGCAGTATAGCCGCTTC	GCCACAATCCGGGCAATCT
Human	*Nrf2*	AGCACATCCAGTCAGAAACC	GTAGCCGAAGAAACCTCATTG
Human	*Keap1*	GGGAGGTGGCCAAGCAAGAGG	TCACCTGCGTGGGCTTGTGCAG
Human	*Cul3*	AGAGCGGAAAGGAGAAGTCGTAGA	CTCAAAGTCACCCGCAATAGTT
Human	*Cat*	AACACTGCCAATGATGATAACG	TCTTGACCGCTTTCTTCTGG
Human	*Sod1*	CGAGCAGAAGGAAAGTAATG	TGGATAGAGGATTAAAGTGAGG
Human	*Gpx1*	GTGCTCGGCTTCCCGTGCAAC	CTCGAAGAGCATGAAGTTGGGC
Mouse	*β-actin*	GGCTGTATTCCCCTCCATCG	CCAGTTGGTAACAATGCCATGT
Mouse	*iNOS*	GTTCTCAGCCCAACAATACAAGA	GTGGACGGGTCGATGTCAC-3
Mouse	*IL-1β*	GCAACTGTTCCTGAACTCAACT	ATCTTTTGGGGTCCGTCAACT
Mouse	*IL-6*	TAGTCCTTCCTACCCCAATTTCC	TTGGTCCTTAGCCACTCCTTC
Mouse	*TNF-α*	CCCTCACACTCAGATCATCTTCT	GCTACGACGTGGGCTACAG
Mouse	*Jak2*	TTGTGGTATTACGCCTGTGTATC	ATGCCTGGTTGACTCGTCTAT
Mouse	*Stat3*	CAATACCATTGACCTGCCGAT	GAGCGACTCAAACTGCCCT
Mouse	*Nrf2*	TCAGCAGCATCCTCTCCAC	GGTCACAGCCTTCAATAGTCC
Mouse	*Keap1*	GGCGGCAGAAGAAGTCATC	TGGTGGTGGGAGTTCAAGG
Mouse	*Cul3*	TCCCACCAGCACCAAGAC	CACCGCCAACACCAACC
Mouse	*Cat*	CTTCTGGAGTCTTCGTC	GGTCGGTCTTGTAATGG
Mouse	*Sod1*	CGAGCAGAAGGCAAGC	ATGTTTCTTAGAGTGAGG
Mouse	*Gpx1*	CGCTCTTTACCTTCCTGCGGAA	AGTTCCAGGCAATGTCGTTGCG

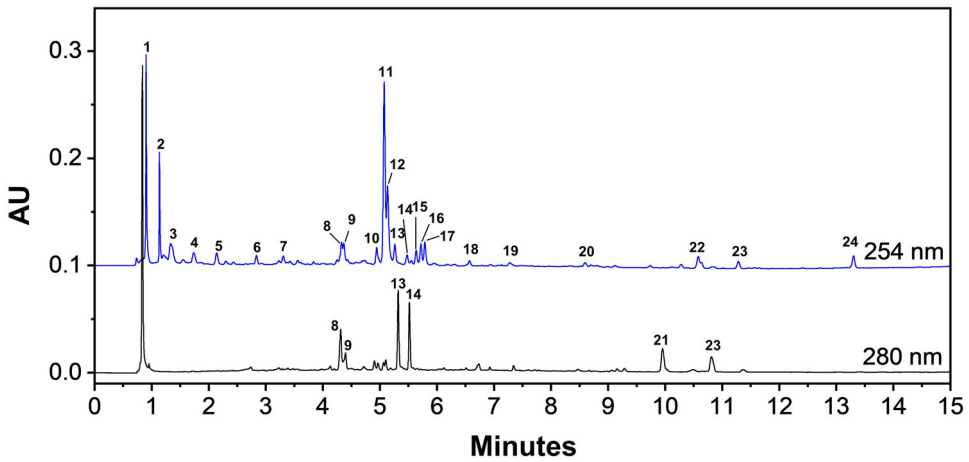


FIGURE 1 | UPLC chromatogram of loquat leaf hair.

including 21 polyphenols were identified by the combination of standard substances and ion fragments (Bell et al. 2015; Bhattarai et al. 2020; Brito et al. 2021; Dulf et al. 2015; Koolen et al. 2017; G. Liu et al. 2021; Mahmoud et al. 2014; Park et al. 2019; Qiao et al. 2021; Rainha et al. 2013; Rasheed et al. 2013; Sayed et al. 2022; Simonetti et al. 2019; Wang et al. 2017; Xie et al. 2010; Yao et al. 2021; J. Zhang et al. 2022), including 15 flavonoids, 4 phenolic acids, 1 coumarin, 1 procyanidin,

TABLE 2 | Determination of phenolics and other compounds in loquat leaf hairs.

Peak no.	TR (min)	[M-H]$^-$(m/z)	Fragment ions (m/z)	Formula	Tentative compounds	References
1	0.9015	191.0583	191.0552 ($C_7H_{11}O_6^-$), 173.0441 ($C_7H_9O_5^-$), 127.0406 ($C_6H_7O_3^-$), 85.0325 ($C_3HO_3^-$)	$C_7H_{12}O_6$	Quinic acid*	Simonetti et al. (2019)
2	1.1356	243.0623	200.0555 ($C_7H_9N_2O_5^-$), 110.0289 ($C_4H_3N_2O_2^-$)	$C_9H_{12}N_2O_6$	Uridine*	Koolen et al. (2017)
3	1.3406	282.0857	150.0417 ($C_5H_4N_5O^-$), 133.0153 ($C_5H_9O_4^-$), 108.0208 ($C_4H_2N_3O^-$)	$C_{10}H_{13}N_5O_5$	Isoguanosine	Bhattarai et al. (2020)
4	1.7371	299.078	137.0249 ($C_7H_5O_3^-$), 93.0370 ($C_6H_5O^-$)	$C_{13}H_{16}O_8$	4-*O*-Glucosyl-4-hydroxybenzoic acid	G. Liu et al. (2021)
5	2.1388	353.0887	191.0564 ($C_7H_{11}O_6^-$), 179.0354 ($C_9H_7O_4^-$), 135.0456 ($C_8H_7O_2^-$)	$C_{16}H_{18}O_9$	Chlorogenic acid*	Rainha et al. (2013)
6	2.8355	325.0935	163.0409 ($C_9H_7O_3^-$), 119.0492 ($C_4H_7O_4^-$)	$C_{15}H_{18}O_8$	*p*-Coumaric acid-4-*O*-glucoside*	Sayed et al. (2022)
7	3.3065	577.1356	425.0893 ($C_{22}H_{17}O_9^-$), 407.0819 ($C_{22}H_{15}O_8^-$), 289.0733 ($C_{15}H_{13}O_6^-$)	$C_{30}H_{26}O_{12}$	Procyanidin B2*	Yao et al. (2021)
8	4.3288	433.1148	343.0842 ($C_{18}H_{15}O_7^-$), 313.0736 ($C_{17}H_{13}O_6^-$)	$C_{21}H_{22}O_{10}$	Prunin*	J. Zhang et al. (2022)
9	4.3648	625.142	463.0895 ($C_{21}H_{19}O_{12}^-$), 301.0365 ($C_{15}H_9O_7^-$)	$C_{27}H_{30}O_{17}$	Baimaside*	Brito et al. (2021)
10	4.9448	609.1473	301.0371 ($C_{15}H_9O_7^-$)	$C_{27}H_{30}O_{16}$	Rutin*	Rasheed et al. (2013)
11	5.075	463.0888	301.0353 ($C_{15}H_9O_7^-$), 151.0035 ($C_7H_3O_4^-$)	$C_{21}H_{20}O_{12}$	Isoquercitrin*	Dulf et al. (2015)
12	5.1329	475.1249	415.1091 ($C_{21}H_{19}O_9^-$), 295.0614 ($C_{13}H_{11}O_8^-$), 175.0025 ($C_6H_7O_6^-$)	$C_{23}H_{24}O_{11}$	Naringenin-6-*C*-(2″-*O*-acetyl)-glucoside	Park et al. (2019)
13	5.2606	579.1725	459.1205 ($C_{19}H_{23}O_{13}^-$), 271.0617 ($C_{15}H_{11}O_5^-$)	$C_{27}H_{32}O_{14}$	Naringin*	Wang et al. (2017)
14	5.4754	609.1843	343.0750 ($C_{18}H_{15}O_7^-$), 301.0729 ($C_{16}H_{13}O_6^-$)	$C_{28}H_{34}O_{15}$	Hesperidin*	Wang et al. (2017)
15	5.6346	609.1842	301.0721 ($C_{16}H_{13}O_6^-$)	$C_{28}H_{34}O_{15}$	Neohesperidin*	Wang et al. (2017)
16	5.7187	463.1246	301.0731 ($C_{16}H_{13}O_6^-$), 271.0246 ($C_{15}H_{11}O_5^-$)	$C_{22}H_{24}O_{11}$	Hesperetin-7-*O*-glucoside	Qiao et al. (2021)
17	5.7878	477.105	315.0530 ($C_{16}H_{11}O_7^-$), 299.0203 ($C_{16}H_{11}O_6^-$), 285.0411 ($C_{15}H_9O_6^-$)	$C_{22}H_{22}O_{12}$	Isorhamnetin-3-*O*-glucoside	Bell et al. (2015)
18	6.5695	261.1122 ([M + H]$^+$(m/z))	189.0549 ($C_{11}H_9O_3^+$)	$C_{15}H_{16}O_4$	Auraptenol*	Xie et al. (2010)
19	7.2786	559.1468	489.3598 ($C_{23}H_{21}O_{12}^-$), 357.2096 ($C_{15}H_{17}O_{10}^-$) 285.2233 ($C_{16}H_{13}O_5^-$)	$C_{27}H_{28}O_{13}$	Naringenin-6-*C*-(2″,4″,6″-*O*-triacetyl)-glucoside	Park et al. (2019)
20	8.5958	373.1287 ([M + H]$^+$(m/z))	343.0811 ($C_{19}H_{19}O_6^+$), 315.0869 ($C_{17}H_{15}O_6^+$)	$C_{20}H_{20}O_7$	Isosinensetin*	Wang et al. (2017)

(Continues)

TABLE 2 | (Continued)

Peak no.	TR (min)	$[M-H]^-$(m/z)	Fragment ions (m/z)	Formula	Tentative compounds	References
21	10.5804	403.139 ($[M+H]^+$(m/z))	373.0914 ($C_{20}H_{21}O_7^+$), 211.0243 ($C_{10}H_{11}O_5^+$)	$C_{21}H_{22}O_8$	Nobiletin*	Wang et al. (2017)
22	10.6356	433.1497 ($[M+H]^+$(m/z))	403.1024 ($C_{21}H_{23}O_8^+$), 385.0928 ($C_{20}H_{17}O_8^+$), 345.0615 ($C_{18}H_{17}O_7^+$)	$C_{22}H_{24}O_9$	3,5,6,7,8,3',4'-Heptamethoxyflavone	Wang et al. (2017)
23	11.2841	373.1285 ($[M+H]^+$(m/z))	343.0815 ($C_{19}H_{19}O_6^+$), 211.0243 ($C_{10}H_{11}O_5^+$)	$C_{20}H_{20}O_7$	Tangeretin*	Wang et al. (2017)
24	13.3016	149.0237 ($[M+H]^+$(m/z))	121.0292 ($C_7H_5O_2^+$)	$C_8H_4O_3$	Phthalic anhydride	Mahmoud et al. (2014)

*Indicated that this compound has been compared with standard substances.

1 organic acid, and 2 nucleotides and derivatives. Among the 15 flavonoids, 7 flavanones (prunin, naringenin-6-*C*-(2″-*O*-acetyl)-glucoside, naringin, hesperidin, neohesperidin, hesperetin-7-*O*-glucoside, and naringenin-6-*C*-(2″,4″,6″-*O*-triacetyl)-glucoside), 4 flavonols (baimaside, rutin, isoquercitrin, and isorhamnetin-3-*O*-glucoside), and 4 flavones (isosinensetin, nobiletin, 3,5,6,7,8,3′,4′-heptamethoxyflavone and tangeretin) were included. It was worth mentioning that the four flavones identified from LLH were polymethoxyflavones, which mainly distributed in citrus peel and leaves. Due to their unique anabolism, these substances were mainly distributed in citrus peel and leaves, but less in other plants. Particularly noteworthy is the identification of four polymethoxyflavones—substances previously thought to be predominantly found in citrus peels and leaves—now detected for the first time in loquat leaves, highlighting the distinctive phytochemical profile of LLH.

3.2 | Loquat Leaf Hair Extracts Inhibited LPS-Induced NO Release in L02 Cells

To explore the anti-inflammatory effect of LLH, we established an LPS-induced nitric oxide (NO) release model using L02 cells. As shown in Figure 2A, within the treatment range (12.5~200 μg/mL), the cell viability of all treatment groups was higher than 90%, indicating that the LLH extract did not show significant cytotoxicity to cells. Under the combined effect of LLH and LPS, LLH pretreatment at 200 μg/mL showed a significant decrease in cell viability. To prevent the effect of decreased cell viability on NO release, we chose 100 μg/mL as the upper limit concentration for subsequent experiments. As shown in Figure 2B, when cells were treated with LLH alone, no effect was shown to induce NO release in any concentration range. Compared with the control group, LPS significantly induced the content of NO in the medium, while pretreatment with LLH could significantly reduce the NO concentration, indicating that LLH had a significant inhibitory effect on the NO-inducing effect of LPS. Studies have shown that IL-1β, IL-6, and TNF-α are closely related to LPS-induced inflammation. It was found by ELISA that LPS significantly induced the production and accumulation of IL-1β, IL-6, and TNF-α, while pretreatment with LLH significantly reduced the production and accumulation of IL-1β, IL-6, and TNF-α (Figure 2C). The concentrations of the three inflammatory factors in the cells were inhibited, and all three treatment concentrations had significant effects. The above results indicated that LLH could inhibit the production and accumulation of inflammatory factors induced by LPS.

To explore the mechanism of LPS-induced NO release and cytokines, the mRNA expression of *inducible nitric oxide synthase* (*iNOS*) and cytokines were detected. As shown in Figure 3A, LPS significantly induced the expression of *iNOS*, *IL-1β*, *IL-6*, and *TNF-α*, while pretreatment with LLH could significantly inhibit the upregulation of these genes. Among all the treatment concentrations, 100 μg/mL treatment had the best effect, which inhibited 97.9% (*iNOS*), 94.2% (*IL-1β*), 98.5% (*IL-6*), and 77.35% (*TNF-α*). The Jak2–Stat3 pathway is an important inflammatory regulatory pathway that senses LPS and induces the expression of inflammatory factors through phosphorylation activation cascades. As shown in Figure 3B,C,

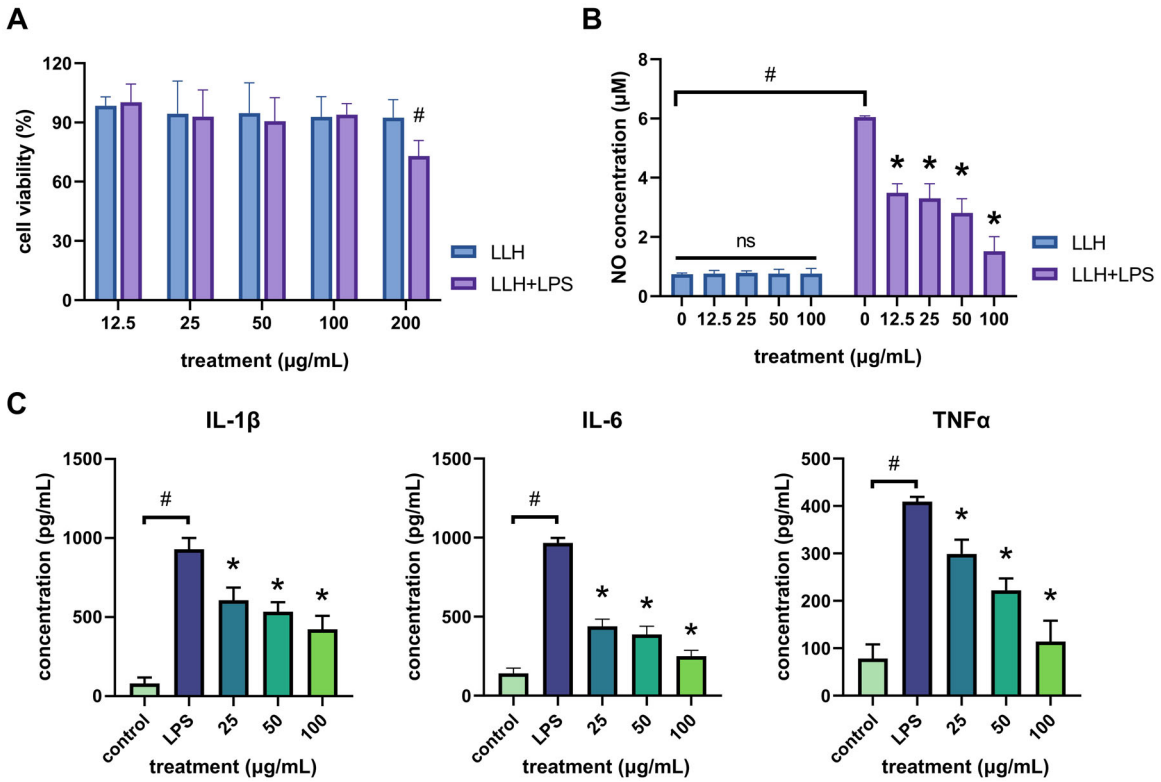


FIGURE 2 | Inhibition of NO release in L02 cells by LLH. (A) Cell viability of L02 cells treated with LLH and LPS; (B) NO concentration detection; (C) concentration of IL-1beta, IL-6, and TNF-α detected by ELISA. * represents significant difference compared to the LPS treatment group and # represents significant difference compared to the control group ($p < 0.05$). Each experiment was repeated three times independently.

LPS could significantly induce the expression of Jak2 and Stat3 at both the transcriptional and protein levels. LLH significantly inhibited the expression of *Jak2* and *Stat3* genes. At the protein level, LLH had no significant effect on the expression of JAK2 protein, but significantly inhibited the phosphorylation level of JAK2 protein. As for the protein expression and phosphorylation level of STAT3, LLH played a significant inhibitory role.

3.3 | Antioxidant Capacity of Loquat Leaf Hair Extracts and Its Protective Effects In Vitro

To further elucidate the antioxidant potential of LLH, both chemical assays and cellular models were used. As shown in Table 3, LLH displayed notable In Vitro antioxidant capacities in four complementary assays (ABTS, DPPH, FRAP, and ORAC). Among these, DPPH scavenging activity was the most pronounced (164.61 ± 2.61 mg Trolox/g FW), whereas FRAP showed a comparatively lower value (26.01 ± 1.70 mg Trolox/g FW), suggesting that LLH may be more efficient in quenching free radicals than in reducing ferric ions.

To further understand the antioxidant mechanism of LLH under inflammatory conditions, we evaluated its effects on LPS induced oxidative stress In Vitro. As illustrated in Figure 4, LPS challenge caused a marked increase in intracellular ROS production and a concomitant decrease in the activities of critical antioxidant enzymes (CAT, SOD, and GSH-Px). These changes were consistent with a downregulation of *Cat*, *Sod1*, and *Gpx1* at the transcriptional level, as well as dysregulation of *Nrf2–Keap1–Cul3*, a key pathway controlling cellular redox homeostasis. Notably, LLH pretreatment effectively attenuated ROS accumulation (Figure 4A), elevated antioxidant enzyme activities (Figure 4B), and restored their mRNA expression (Figure 4C). Moreover, LLH supplementation normalized *Nrf2* transcript levels while suppressing *Keap1*, thereby preserving the overall antioxidant capacity of L02 cells (Figure 4D). The expression of *Cul3* remained relatively unchanged across different treatment groups (Figure 4D). These findings suggest that LLH may alleviate LPS induced oxidative stress by activating the Nrf2–Keap1 pathway and upregulating antioxidant-related genes. Taken together, these findings reinforce the notion that the potent chemical antioxidant activities of LLH, as demonstrated by the multiple In Vitro assays, underpin its protective effects against LPS-induced oxidative damage in liver cells.

3.4 | Loquat Leaf Hair Extracts Inhibited LPS-Induced Inflammatory Factors in C57BL/6J Mouse Liver

To evaluate the anti-inflammatory potential of LLH In Vivo, we employed a C57BL/6 J mouse model of LPS-induced liver inflammation and measured various cytokines in liver tissue. As shown in Figure 5A, intraperitoneal injection of LPS markedly elevated IL-1β (8.68-fold), IL-6 (6.54-fold), and TNF-α (7.59-fold) compared with the control group. By contrast, oral administration of LLH significantly reduced these cytokine levels, underscoring its ability to mitigate LPS-induced inflammation In Vivo. Unlike the cell-based

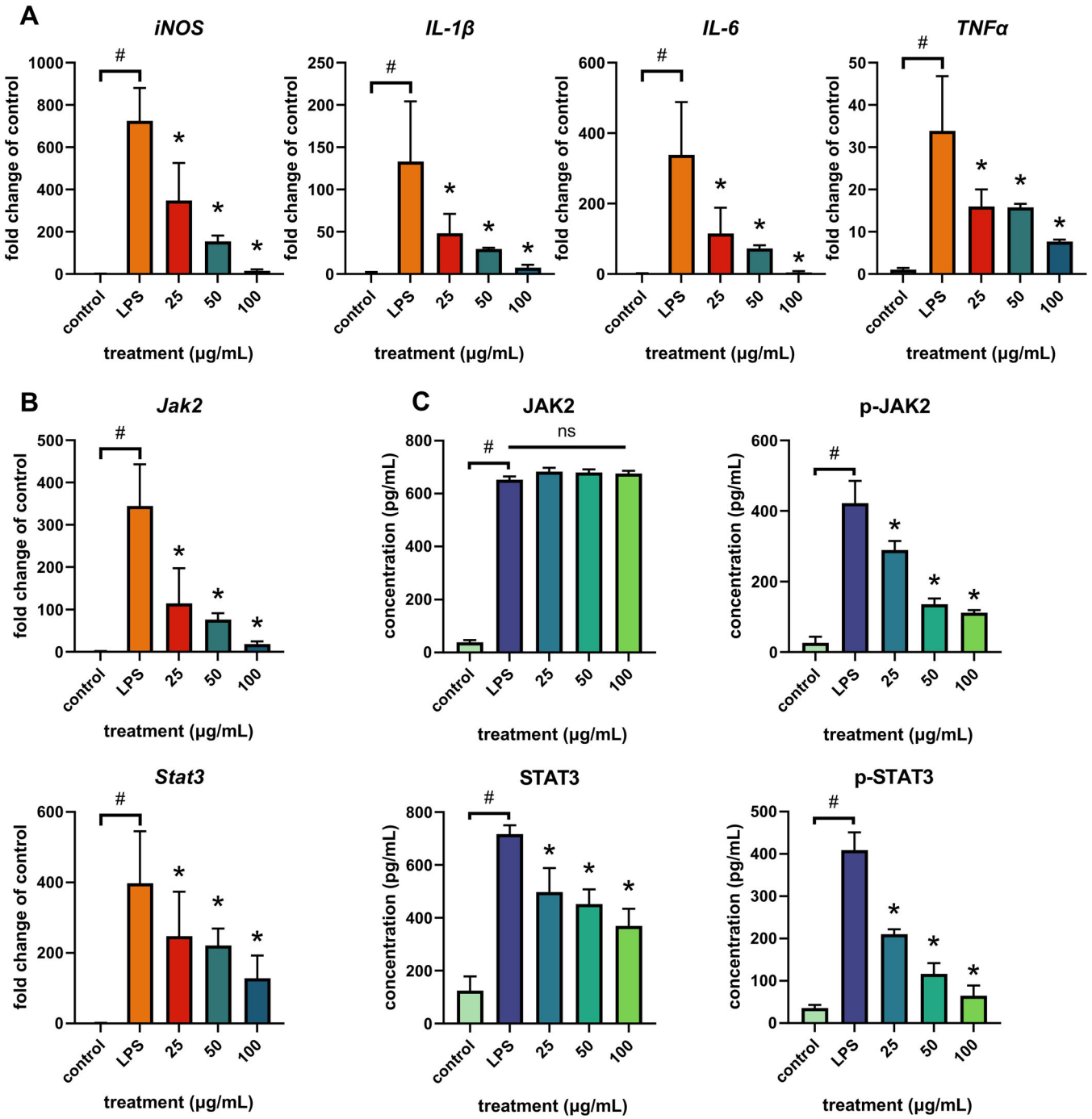


FIGURE 3 | Ameliorating effects of LLH on LPS-induced inflammation in L02 cell lines. (A) Relative gene expression of *iNOS* and cell cytokines detected by qRT-PCR. (B) Relative gene expression of *Jak2* and *Stat3* detected by qRT-PCR. (C) Protein expression and phosphorylation of JAK2 and STAT3 detected by ELISA. * represents significant difference compared to the LPS treatment group and # represents significant difference compared to the control group ($p < 0.05$). Each experiment was repeated three times independently.

findings, however, IL-6 and TNF-α did not consistently exhibit a clear dose-dependent response. Notably, IL-6 levels in the 50 mg/kg·bw·d group were slightly lower than those in the 100 mg/kg·bw·d group.

At the transcriptional level (Figure 5B), LPS markedly upregulated *IL-1β*, *IL-6*, and *TNF-α* genes, whereas LLH administration significantly blunted this induction. Gene and protein analyses of Jak2 and Stat3 (Figure 5C,D) revealed that LPS enhanced both transcription and phosphorylation of these key signaling mediators, while LLH effectively downregulated their expression and phosphorylation. Consequently, the Jak2–Stat3 pathway was suppressed, thereby inhibiting LPS-driven inflammatory responses. Of note, in contrast to our In Vitro observations, LLH not only reduced phosphorylated JAK2 but also diminished total JAK2 protein In Vivo, indicating a potentially stronger inhibitory effect under physiological conditions.

TABLE 3 | Determination of chemical antioxidant capacities loquat leaf hairs.

	Antioxidant capacity (mg Trolox/g FW)
ABTS	54.53 ± 8.58
DPPH	164.61 ± 2.61
FRAP	26.01 ± 1.70
ORAC	65.72 ± 6.08

3.5 | Loquat Leaf Hair Extracts Mitigates LPS-Induced Oxidative Stress in C57BL/6J Mouse Liver

Building on the observed In Vivo anti-inflammatory activity of LLH extracts, we further examined their antioxidant properties in a C57BL/6J mouse model of LPS-induced liver injury (Figure 6). Intraperitoneal injection of LPS markedly reduced the activities of key antioxidant enzymes (CAT, SOD, and GSH-Px) in the liver (Figure 6A), reflecting pronounced

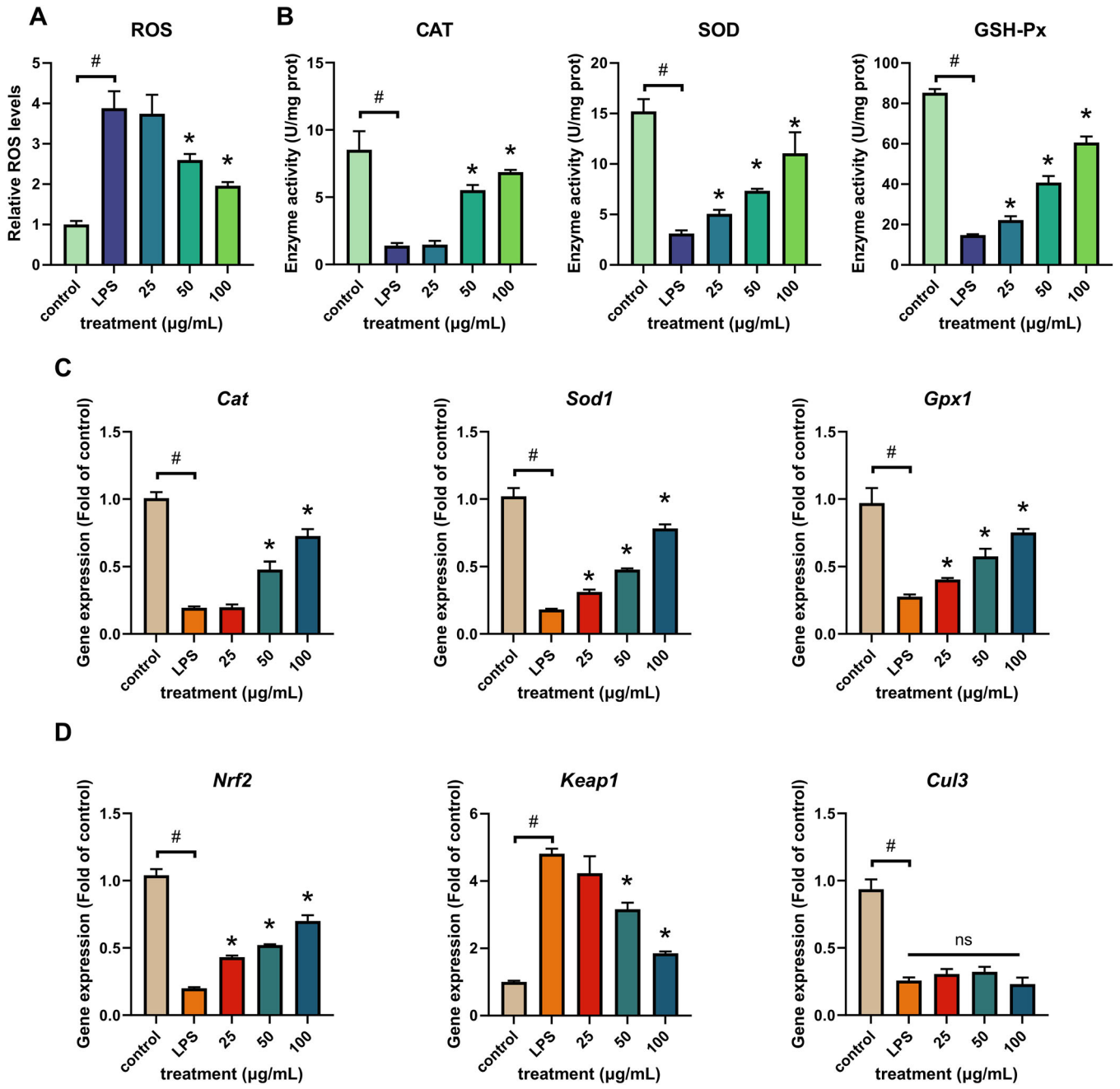


FIGURE 4 | Antioxidant effects of LLH on LPS-induced oxidative stress In Vitro. (A) ROS contents detected by DCFH-DA. (B) Enzyme activities of CAT, SOD, GSH-Px. (C) Relative gene expression of *Cat*, *Sod1*, and *Gpx1* detected by qRT-PCR. (D) Relative gene expression of *Nrf2*, *Keap1*, and *Cul3* detected by qRT-PCR. * represents significant difference compared to the LPS treatment group and # represents significant difference compared to the control group ($p < 0.05$). Each experiment was repeated three times independently.

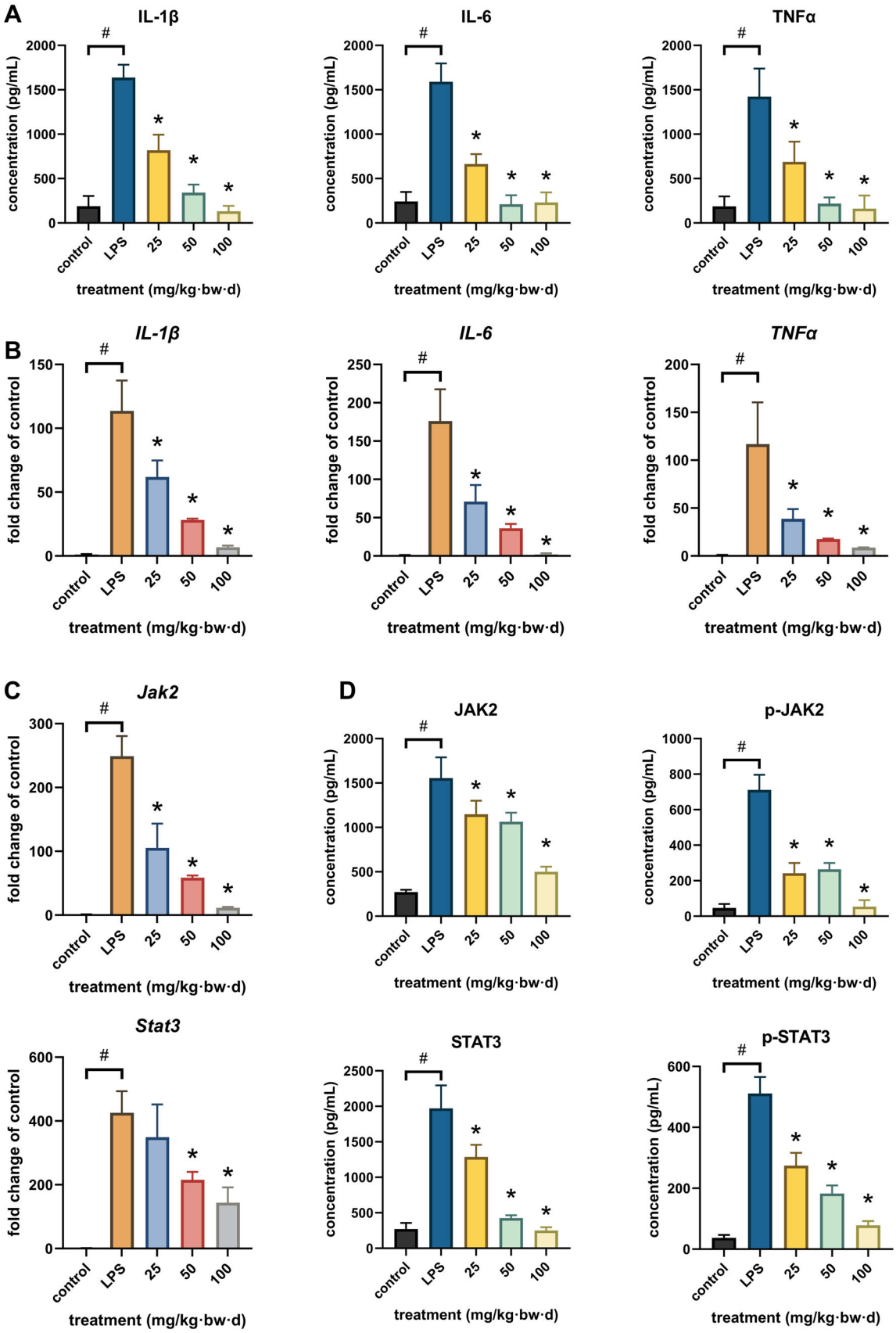


FIGURE 5 | Inhibition of liver inflammation cytokines in C57 mouse by LLH treatments. (A) Concentration of IL-1beta, IL-6, and TNF-α detected by ELISA. (B) Relative gene expression of *iNOS* and cell cytokines detected by qRT-PCR. (C) Relative gene expression of *Jak2* and *Stat3* detected by qRT-PCR. (D) Protein expression and phosphorylation of JAK2 and STAT3 detected by ELISA. * represents significant difference compared to the LPS treatment group and # represents significant difference compared to the control group ($p < 0.05$). Each treatment consisted of five biological replicates.

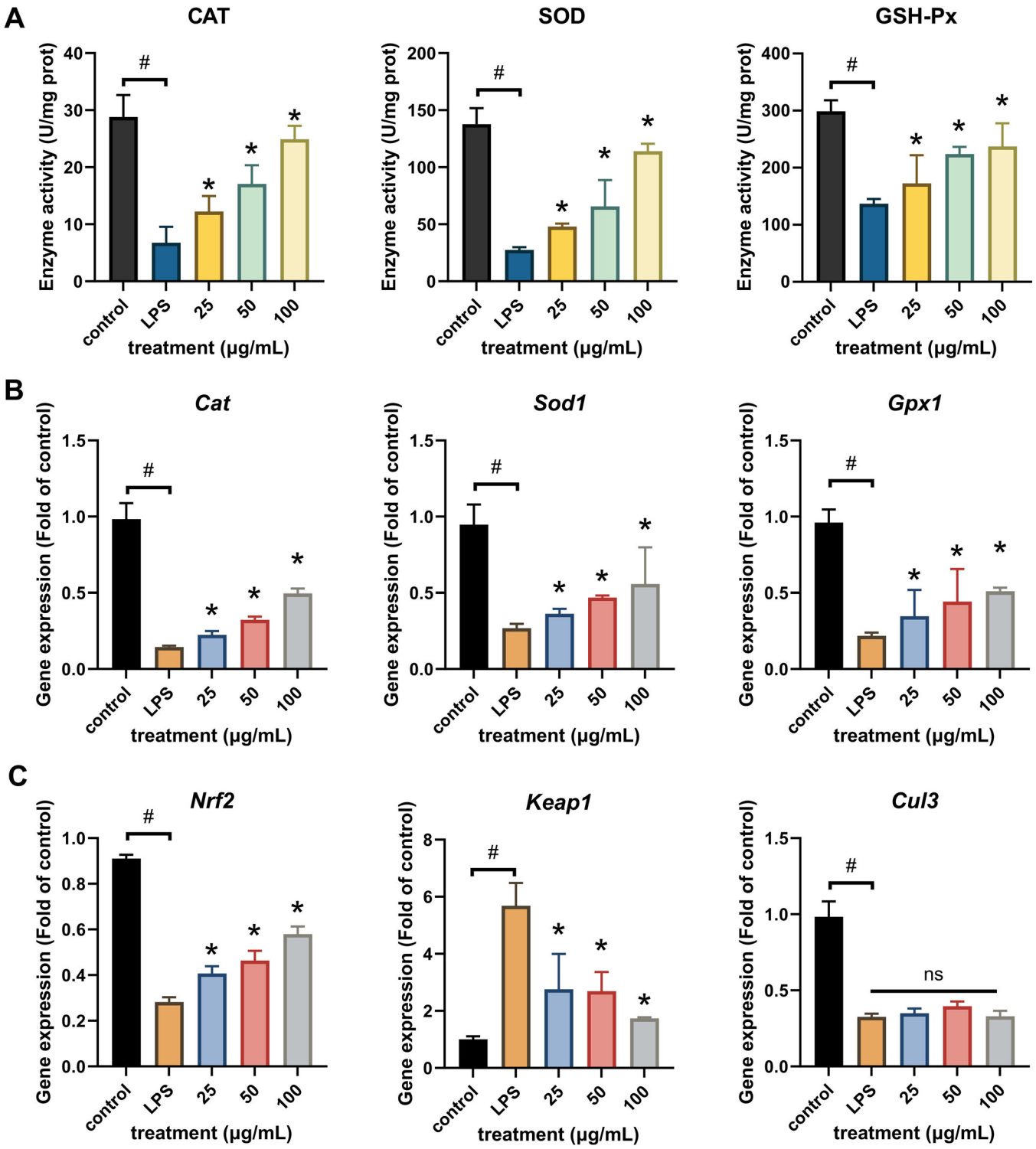


FIGURE 6 | Antioxidant effects of LLH on LPS-induced oxidative stress In Vivo. (A) Enzyme activities of CAT, SOD, GSH-Px in C57 mice liver. (B) Relative gene expression of *Cat*, *Sod1*, and *Gpx1* detected by qRT-PCR. (C) Relative gene expression of *Nrf2*, *Keap1*, and *Cul3* detected by qRT-PCR. * represents significant difference compared to the LPS treatment group and # represents significant difference compared to the control group ($p < 0.05$). Each treatment consisted of five biological replicates.

oxidative damage. However, oral administration of LLH at 25, 50, and 100 mg/kg significantly restored these enzyme activities, with the 100 mg/kg dose exhibiting the strongest effect, indicating a dose-dependent improvement in liver antioxidant capacity.

Similar trends were observed at the transcriptional level (Figure 6B). LPS challenge downregulated *Cat*, *Sod1*, and *Gpx1* genes, whereas LLH treatment upregulated their expression, suggesting that LLH promotes the synthesis of antioxidant enzymes by modulating gene transcription. This enhanced

enzymatic activity likely fortifies the liver's defense against oxidative stress.

Regarding the Nrf2–Keap1 axis (Figure 6C), LPS significantly downregulated *Nrf2* while upregulating *Keap1*. By contrast, LLH reversed these changes, increasing *Nrf2* expression and decreasing *Keap1* levels. *Cul3* expression remained relatively stable across all groups. These findings imply that LLH activates the *Nrf2–Keap1* pathway In Vivo, thereby augmenting antioxidant gene expression and enzymatic functions.

Notably, these improvements in hepatic oxidative status were accompanied by diminished inflammatory responses. In tandem with bolstered antioxidant defenses, LLH-treated mice exhibited lower concentrations of pro-inflammatory cytokines (IL-1β, IL-6, and TNF-α) relative to the LPS-only group. Collectively, these results underscore the strong antioxidant capacity of LLH and its potent protective effects against LPS-induced oxidative damage and inflammation in mouse liver.

4 | Discussion

Previous studies on loquat (*Eriobotrya japonica* (*E. japonica*)) leaves have primarily focused on bioactive components in the mesophyll, such as chlorogenic acid, ursolic acid, and flavonoids like rutin and isoquercitrin, which are linked to antioxidant and anti-inflammatory activities (Xiao et al. 2023; Xu et al. 2014). However, the dense trichomes (leaf hairs) covering the abaxial surface of loquat leaves—a tissue distinct from the mesophyll—have remained uncharacterized in terms of their phytochemical composition and biological effects. While plant trichomes are recognized as sites of natural product enrichment, particularly for specialized metabolites like polyphenols (Y. Liu et al. 2019), no prior reports have addressed the chemical profile or bioactivities of LLH.

This study fills this gap by demonstrating that LLH contains a unique suite of polyphenols. Among the substances identified this time, 10 were previously identified in loquat, while 14 were identified for the first time in loquat, including four polymethoxyflavones (isosinensetin, nobiletin, 3,5,6,7,8,3′,4′-heptamethoxyflavone, and tangeretin)—compounds previously thought to be exclusive to citrus peels and leaves (Wang et al. 2022). Unlike the hydroxycinnamic acids and flavonols dominant in loquat mesophyll, these polymethoxyflavones possess multiple methoxy groups. These structural differences in polyphenols—hydroxyl-rich flavonols in mesophyll versus methoxy-rich polymethoxyflavones in leaf hairs—are rooted in distinct biosynthetic pathways. Flavonols like rutin and isoquercitrin arise from the canonical phenylpropanoid pathway, where chalcone synthase (CHS) and chalcone isomerase (CHI) first assemble the flavonoid backbone, followed by hydroxylation at the C3 position by flavanone 3-hydroxylase (F3H) and glycosylation by UDP-glycosyltransferases (UGTs) (L. Zhang et al. 2017). This pathway prioritizes hydroxyl group addition, enabling hydrogen bonding and hydrophilic interactions that underlie their antioxidant activities in aqueous cellular environments. However, the key to PMF biosynthesis are successive *O*-methylation reactions mediated by *O*-methyltransferases (OMTs), which introduce methoxy groups (–OCH_3) at multiple positions (e.g., C-6, C-7, C-8, C-3′, C-4′) on the flavanone nucleus, distinguishing PMFs from other flavonoids. Hydroxylation by enzymes like F3H provides precursor substrates for methylation, while glycosylation or acylation modifications are relatively rare, emphasizing the primacy of methoxylation in PMF structure (Zhu et al. 2023). This is the first time that polymethoxyflavones have been found in fruit trees other than citrus. These results suggest that the active substances in LLH differ significantly from those in loquat mesophyll.

Loquat leaves are a folk food-medicine homologous product with anti-inflammatory activity. However, in previous studies, the anti-inflammatory effect of loquat leaves was attributed to the extract or active substances of the whole loquat leaf. For example, Jian et al. (2020) reported that the flavonoid extract of loquat leaves could inhibit chronic obstructive pulmonary disease induced by cigarette smoke. Oral administration of 50 or 100 mg/kg/day of loquat flavonoids could suppress the accumulation of IL-6, IL-1β, TNF-α and promote the activity of antioxidant enzyme SOD. Wu et al. (2022) also found that loquat leaf extracts and one of the active substances sesquiterpene glycosides could regulate intestinal flora, inhibit hyperglycemia and inflammatory cytokine release in db/db mice. T. Kim et al. (2020) found that the aqueous extract of loquat leaves could effectively inhibit asthma induced by ovalbumin, the release of NO in human tracheal smooth muscle cells, and the expression of inflammatory factors. Kumar et al. (2024) reviewed the phytochemical potential of loquat and specifically mentioned the antioxidant, anti-inflammatory and antidiabetic effects of the flavonoid compounds in loquat. However, previous studies on the biological efficacy of LLH have not been carried out. Whether the loquat hair has the effect of inhibiting inflammation has not been known before. In our study, the effect of loquat hair extract on LPS-induced liver inflammation was evaluated using two model carriers, L02 cells and C57BL/6J mice. It was found that the loquat hair extract could inhibit the release of NO induced by LPS, and suppress the expression of inflammatory cytokine genes and proteins. The anti-inflammatory activity of LLH extract may be related to the substances contained in it, especially the polymethoxyflavones in loquat hair such as nobiletin, tangeretin, etc., exhibited similar effects of inhibiting LPS-induced NO release and inflammatory factor expression (Wang et al. 2019).

Loquat and citrus, both celebrated as medicine-food homology fruits, exhibit striking parallels in their antioxidant and anti-inflammatory profiles, despite belonging to distinct plant families (Rosaceae vs. Rutaceae). Both taxa harness polyphenolic compounds to combat oxidative stress: their extracts scavenge ROS, activate the Nrf2-mediated antioxidant pathway, and enhance the activity of enzymes like SOD and glutathione peroxidase (GSH-Px)—mechanisms critical for maintaining redox homeostasis (Kumar et al. 2024; Wang et al. 2021, 2022; Yan et al. 2023). In the realm of inflammation, both fruits demonstrate the ability to suppress LPS-induced NO overproduction, a hallmark of excessive immune activation, while modulating key signaling cascades such as Jak2–Stat3, NF-κB, and PPARs to dampen pro-inflammatory cytokine release (e.g., IL-6, TNF-α) (Kumar et al. 2024; Wang et al. 2019). These shared effects suggest a conserved functional framework for polyphenol-mediated health benefits across divergent plant lineages. Notably, their bioactive

potentials are anchored in distinct tissue niches: citrus relies on peel-enriched polymethoxyflavones (PMFs) to exert protective effects, whereas loquat has traditionally utilized leaf mesophyll compounds like chlorogenic acid. Our discovery of PMFs in LLH—structurally akin to those in citrus peels but residing in a different organ—introduces an intriguing hypothesis: PMFs may serve as a shared molecular bridge underlying the "medicine–food homology" of both genera. Despite evolving in separate taxonomic lineages, the accumulation of PMFs in specialized tissues (citrus peel for fruit protection, LLH for foliar defense) might represent a convergent strategy to synthesize lipophilic polyphenols capable of penetrating cellular membranes and engaging conserved inflammatory signaling nodes. This cross-tissue, cross-genera occurrence of PMFs invites reevaluation of their role as pivotal bioactives, potentially unifying the diverse health claims associated with these two iconic fruits and guiding future investigations into the chemical basis of their shared therapeutic effects. The Jak2–Stat3 pathway is one of the main pathways for inflammation regulation, which includes two major proteins: Jak2 and Stat3. When stimuli such as cytokines or growth factors bind to their receptors, the receptor activates Jak2, leading to Jak2 autophosphorylation and activation (Witthuhn et al. 1993). Activated Jak2 then phosphorylates the Stat3 protein inside the cell, allowing it to activate and enter the nucleus. In the nucleus, the activated Stat3 protein can bind to DNA, initiating or inhibiting the transcription of relevant genes, thereby affecting cell function and behavior (Siveen et al. 2014). The Jak2–Stat3 pathway plays an important role in the occurrence and development of various diseases, such as tumors, inflammatory diseases, and autoimmune diseases (Hu et al. 2021). Therefore, the pathway has become a potential target for the treatment of some diseases. Various bioactive substances have been found to have regulatory effects on the Jak2–Stat3 pathway, such as curcumin (Lin et al. 2010), mulberry bark (C. Kim et al. 2016), salvia (Lee et al. 2016), artemisinin (Zeng et al. 2014), etc. Our previous studies also found that citrus extract or polymethoxyflavones monomers could inhibit the occurrence and development of inflammation by regulating the Jak2–Stat3 pathway (Wang et al. 2019). However, in previous studies, it has not been reported whether loquat extract can regulate and inhibit inflammation through the Jak2–Stat3 pathway. In the current study, a notable discrepancy was observed in the regulation of the Jak2–Stat3 pathway between In Vitro and In Vivo models: LLH treatment primarily inhibited p-JAK2/p-STAT3 phosphorylation in L02 cells, whereas it reduced both total JAK2/STAT3 protein expression and phosphorylation in mouse liver tissue. This divergence likely stems from the distinct physiological contexts of the two models. In Vitro, L02 cells represent a homogeneous hepatic cell population with direct exposure to LLH, where the primary action may involve blocking Jak2 kinase activity or interrupting receptor-mediated phosphorylation cascades, without systemic metabolic influences. By contrast, In Vivo, oral administration of LLH subjects the extract to gastrointestinal metabolism and hepatic first-pass effects, potentially enhancing bioactive component delivery to liver tissue and enabling broader regulatory effects—including downregulation of Jak2/Stat3 gene transcription—in addition to inhibiting phosphorylation.

Equally important is the robust antioxidant capacity exhibited by LLH, which not only complements the anti-inflammatory response but can also help mitigate the oxidative damage that typically accompanies chronic inflammation. Our chemical assays (ABTS, DPPH, FRAP, and ORAC) revealed that LLH demonstrates substantial free radical scavenging and ferric-reducing capabilities. In Vitro, LLH significantly suppressed ROS accumulation and bolstered the activity of antioxidant enzymes (CAT, SOD, GSH-Px) in LPS-challenged L02 cells, while upregulating the corresponding genes (*Cat*, *Sod1*, *Gpx1*). The *Nrf2–Keap1* signaling pathway, a central player in orchestrating the cellular antioxidant response, was also favorably modulated by LLH treatment. This upregulation of Nrf2 and downregulation of Keap1 are consistent with an enhanced intracellular antioxidant defense mechanism. The same protective trend was confirmed In Vivo: LLH supplementation countered the LPS-induced decline in enzymatic activity and gene expression of antioxidant mediators in C57BL/6J mouse livers, thereby reducing oxidative liver injury. These results are consistent with previous research suggesting Nrf2 activation as a key molecular mechanism underlying the beneficial effects of polyphenols against oxidative damage (Jeon et al. 2025; Wang et al. 2022).

Collectively, our study not only broadens the phytochemical understanding of LLH but also demonstrates its significant therapeutic potential in inflammation and oxidative stress management through modulation of the *Jak2–Stat3* and *Nrf2–Keap1* signaling pathways. Future research should focus on isolating specific active constituents, exploring synergistic effects between different polyphenols, and conducting clinical trials to evaluate safety and efficacy in human populations. These findings pave the way for innovative applications of LLH in functional food, dietary supplements, and pharmaceutical products, promoting the sustainable and high-value utilization of loquat leaf resources.

5 | Conclusions

In this study, we identified and characterized the polyphenolic composition of loquat (*E. japonica* Lindl.) leaf hair (LLH) using UPLC–HRMS, revealing 24 compounds, including 21 polyphenols, with 4 polymethoxyflavones reported for the first time in loquat leaf. The findings highlight LLH as a rich source of bioactive polyphenols with potential health benefits.

Our results demonstrate that LLH exhibits significant antioxidant and anti-inflammatory activities. Chemical antioxidant assays (ABTS, DPPH, FRAP, and ORAC) confirmed the strong radical-scavenging and reducing capacities of LLH, particularly its high DPPH scavenging ability.

In In Vitro experiments using LPS-stimulated L02 cells, LLH effectively suppressed ROS accumulation, preserved antioxidant enzyme activities (CAT, SOD, and GSH-Px), and upregulated key antioxidant-related genes (*Nrf2, Cat, Sod1, Gpx1*). Additionally, LLH significantly inhibited LPS-induced NO release and pro-inflammatory cytokine (*IL-1β, IL-6, TNF-α*) production while downregulating Jak2–Stat3 pathway activation. These findings suggest that LLH mitigates oxidative stress and inflammation at both cellular and molecular levels.

The In Vivo study using an LPS-induced liver injury model in mice further validated these effects. Oral administration of LLH

significantly reduced oxidative stress by enhancing hepatic antioxidant enzyme activities and restoring *Nrf2*-mediated transcriptional activation. Simultaneously, LLH suppressed LPS-induced inflammatory responses by downregulating cytokine production and Jak2–Stat3 signaling. Notably, the highest LLH dose (100 mg/kg) restored antioxidant and anti-inflammatory markers to near-normal levels, indicating dose-dependent efficacy.

Overall, our findings highlight LLH as a promising natural antioxidant and anti-inflammatory agent capable of modulating oxidative stress and inflammatory pathways. These results provide a foundation for further exploration of LLH as a functional food ingredient or therapeutic candidate for managing inflammation-associated oxidative damage. Future research should focus on isolating key active compounds and investigating their pharmacokinetics and long-term safety in clinical applications.

Author Contributions

Can Hu: conceptualization, writing – original draft, investigation, validation, software, methodology. **Jiazheng Hu:** investigation, visualization, formal analysis. **Hongyu Ye:** validation, formal analysis, data curation. **Mengxin Wang:** investigation, writing – original draft, formal analysis, data curation. **Manxi Wu:** investigation, formal analysis. **Han Yang:** investigation, visualization, resources. **Kang Chen:** resources, data curation. **Jinping Cao:** investigation, writing – review and editing. **Yanshuai Wang:** writing – review and editing, investigation, data curation, software, project administration. **Yue Wang:** supervision, conceptualization, writing – review and editing, funding acquisition, resources. **Chongde Sun:** conceptualization, supervision.

Acknowledgments

This article was supported by the Fundamental Research Funds for the Zhejiang Provincial Universities (226-2024-00211).

Conflicts of Interest

The authors declare no conflicts of interest.

Data Availability Statement

The data that support the findings of this study are available from the corresponding author upon reasonable request.

References

Bell, L., M. J. Oruna-Concha, and C. Wagstaff. 2015. "Identification and Quantification of Glucosinolate and Flavonol Compounds in Rocket Salad (*Eruca sativa*, *Eruca vesicaria* and *Diplotaxis tenuifolia*) by LC–MS: Highlighting the Potential for Improving Nutritional Value of Rocket Crops." *Food Chemistry* 172: 852–861. https://doi.org/10.1016/j.foodchem.2014.09.116.

Bhattarai, S., J. Pippel, E. Scaletti, et al. 2020. "2-Substituted α,β-Methylene-ADP Derivatives: Potent Competitive Ecto-5′-Nucleotidase (CD73) Inhibitors With Variable Binding Modes." *Journal of Medicinal Chemistry* 63, no. 6: 2941–2957. https://doi.org/10.1021/acs.jmedchem.9b01611.

Brito, T. B. N., L. R. S. Lima, M. C. B. Santos, et al. 2021. "Antimicrobial, Antioxidant, Volatile and Phenolic Profiles of Cabbage-Stalk and Pineapple-Crown Flour Revealed by GC-MS and UPLC-MS^{E}." *Food Chemistry* 339: 127882. https://doi.org/10.1016/j.foodchem.2020.127882.

Chen, B., P. Long, Y. Sun, et al. 2017. "The Chemical Profiling of Loquat Leaf Extract by HPLC-DAD-ESI-MS and Its Effects on Hyperlipidemia and Hyperglycemia in Rats Induced by a High-Fat and Fructose Diet." *Food & Function* 8, no. 2: 687–694. https://doi.org/10.1039/c6fo01578f.

Chen, Y., H. Ma, J. Liang, et al. 2024. "Hepatoprotective Potential of Four Fruit Extracts Rich in Different Structural Flavonoids Against Alcohol-Induced Liver Injury via Gut Microbiota-Liver Axis." *Food Chemistry* 460: 140460.

Dulf, F. V., D. C. Vodnar, E. H. Dulf, and M. I. Toşa. 2015. "Total Phenolic Contents, Antioxidant Activities, and Lipid Fractions From Berry Pomaces Obtained by Solid-State Fermentation of Two *Sambucus* Species With *Aspergillus niger*." *Journal of Agricultural and Food Chemistry* 63, no. 13: 3489–3500. https://doi.org/10.1021/acs.jafc.5b00520.

Fajgenbaum, D. C., and C. H. June. 2020. "Cytokine Storm." *New England Journal of Medicine* 383, no. 23: 2255–2273. https://doi.org/10.1056/NEJMra2026131.

Grivennikov, S. I., and M. Karin. 2011. "Inflammatory Cytokines in Cancer: Tumour Necrosis Factor and Interleukin 6 Take the Stage." *Annals of the Rheumatic Diseases* 70: i104–i108. https://doi.org/10.1136/ard.2010.140145.

Hu, X., J. Li, M. Fu, X. Zhao, and W. Wang. 2021. "The JAK/STAT Signaling Pathway: From Bench to Clinic." *Signal Transduction and Targeted Therapy* 6, no. 1: 402. https://doi.org/10.1038/s41392-021-00791-1.

Jeon, Y. A., P. Natraj, S. H. Paik, S. C. Kim, and Y. J. Lee. 2025. "Exploring the Protective Mechanisms of Chayote (*Sechium edule*) Juice in Mitigating Streptozotocin-Induced Pancreatic Dysfunction." *eFood* 6, no. 1: e70036. https://doi.org/10.1002/efd2.70036.

Jian, T., J. Chen, X. Ding, et al. 2020. "Flavonoids Isolated From Loquat (*Eriobotrya japonica*) Leaves Inhibit Oxidative Stress and Inflammation Induced by Cigarette Smoke in COPD Mice: The Role of TRPV1 Signaling Pathways." *Food & Function* 11, no. 4: 3516–3526. https://doi.org/10.1039/c9fo02921d.

Kim, C., J. H. Kim, E. Y. Oh, et al. 2016. "Blockage of STAT3 Signaling Pathway by Morusin Induces Apoptosis and Inhibits Invasion in Human Pancreatic Tumor Cells." *Pancreas* 45, no. 3: 409–419. https://doi.org/10.1097/MPA.0000000000000496.

Kim, T., K. R. Paudel, and D. W. Kim. 2020. "*Eriobotrya japonica* Leaf Extract Attenuates Airway Inflammation in Ovalbumin-Induced Mice Model of Asthma." *Journal of Ethnopharmacology* 253: 112082. https://doi.org/10.1016/j.jep.2019.112082.

Koolen, H. H. F., E. M. F. Pral, S. C. Alfieri, et al. 2017. "Antiprotozoal and Antioxidant Alkaloids From *Alternanthera littoralis*." *Phytochemistry* 134: 106–113. https://doi.org/10.1016/j.phytochem.2016.11.008.

Kumar, V., P. Gupta, and M. Kumar. 2024. "Loquat and Its Phytochemical Potential: A Promising Application in Food Technology." *eFood* 5, no. 3: e158. https://doi.org/10.1002/efd2.158.

Lee, S. J., H. J. Jang, Y. Kim, et al. 2016. "Inhibitory Effects of IL-6-Induced STAT3 Activation of Bio-Active Compounds Derived From *Salvia plebeia* R.Br." *Process Biochemistry* 51, no. 12: 2222–2229. https://doi.org/10.1016/j.procbio.2016.09.003.

Lei, Y., K. Wang, L. Deng, Y. Chen, E. C. Nice, and C. Huang. 2015. "Redox Regulation of Inflammation: Old Elements, a New Story." *Medicinal Research Reviews* 35, no. 2: 306–340. https://doi.org/10.1002/med.21330.

Li, Y., X. Feng, X. Zheng, J. Zhu, and Q. Gu. 2023. "Food-Borne Polyphenols: A Biocompatible Anchor Recuperating Iron Homeostasis." *Food Frontiers* 4, no. 3: 1144–1163. https://doi.org/10.1002/fft2.244.

Lin, L., B. Hutzen, M. Zuo, et al. 2010. "Novel STAT3 Phosphorylation Inhibitors Exhibit Potent Growth-Suppressive Activity in Pancreatic and Breast Cancer Cells." *Cancer Research* 70, no. 6: 2445–2454. https://doi.org/10.1158/0008-5472.CAN-09-2468.

Liu, G., W. Zhu, S. Li, et al. 2021. "Antioxidant Capacity and Interaction of Endogenous Phenolic Compounds From Tea Seed Oil." *Food Chemistry* 376: 131940. https://doi.org/10.1016/j.foodchem.2021.131940.

Liu, Y., S. X. Jing, S. H. Luo, and S. H. Li. 2019. "Non-Volatile Natural Products in Plant Glandular Trichomes: Chemistry, Biological Activities and Biosynthesis." *Natural Product Reports* 36, no. 4: 626–665. https://doi.org/10.1039/c8np00077h.

Mahmoud, E., D. A. Watson, and R. F. Lobo. 2014. "Renewable Production of Phthalic Anhydride From Biomass-Derived Furan and Maleic Anhydride." *Green Chemistry* 16, no. 1: 167–175. https://doi.org/10.1039/c3gc41655k.

Park, B. J., T. Nomura, H. Fukudome, M. Onjo, A. Shimada, and H. Samejima. 2019. "Chemical Constituents of the Leaves of *Eriobotrya japonica*." *Chemistry of Natural Compounds* 55, no. 5: 942–944. https://doi.org/10.1007/s10600-019-02854-w.

Qiao, R., L. Zhou, M. Zhong, et al. 2021. "Spectrum-Effect Relationship Between UHPLC-Q-TOF/MS Fingerprint and Promoting Gastrointestinal Motility Activity of *Fructus aurantii* Based on Multivariate Statistical Analysis." *Journal of Ethnopharmacology* 279: 114366. https://doi.org/10.1016/j.jep.2021.114366.

Qiu, P., Q. Wang, X. Li, et al. 2025. "Purple Yam Anthocyanin Forestalling Lipopolysaccharide-Induced Intestine Damage by Selectively Promoting *Lactococcus*." *Food Frontiers*. https://doi.org/10.1002/fft2.546.

Rainha, N., K. Koci, A. V. Coelho, E. Lima, J. Baptista, and M. Fernandes-Ferreira. 2013. "HPLC-UV-ESI-MS Analysis of Phenolic Compounds and Antioxidant Properties of *Hypericum undulatum* Shoot Cultures and Wild-Growing Plants." *Phytochemistry* 86: 83–91. https://doi.org/10.1016/j.phytochem.2012.10.006.

Rasheed, D. M., S. M. El Zalabani, M. A. Koheil, H. M. El-Hefnawy, and M. A. Farag. 2013. "Metabolite Profiling Driven Analysis of *Salsola* Species and Their Anti-Acetylcholinesterase Potential." *Natural Product Research* 27, no. 24: 2320–2327. https://doi.org/10.1080/14786419.2013.832676.

Ratanji, K. D., J. P. Derrick, R. J. Dearman, and I. Kimber. 2014. "Immunogenicity of Therapeutic Proteins: Influence of Aggregation." *Journal of Immunotoxicology* 11, no. 2: 99–109. https://doi.org/10.3109/1547691X.2013.821564.

Santos Tozin, L. R. D., S. C. de Melo Silva, and T. M. Rodrigues. 2016. "Non-Glandular Trichomes in Lamiaceae and Verbenaceae Species: Morphological and Histochemical Features Indicate More Than Physical Protection." *New Zealand Journal of Botany* 54, no. 4: 446–457. https://doi.org/10.1080/0028825x.2016.1205107.

Sayed, A. M. E., F. A. Omar, M. M. A. A. Emam, and M. A. Farag. 2022. "UPLC-MS/MS and GC-MS Based Metabolites Profiling of *Moringa oleifera* Seed With Its Anti-*Helicobacter pylori* and Anti-Inflammatory Activities." *Natural Product Research* 36, no. 24: 6433–6438. https://doi.org/10.1080/14786419.2022.2037088.

Simonetti, G., C. Palocci, A. Valletta, et al. 2019. "Anti-*Candida* Biofilm Activity of Pterostilbene or Crude Extract From Non-Fermented Grape Pomace Entrapped in Biopolymeric Nanoparticles." *Molecules* 24, no. 11: 2070. https://doi.org/10.3390/molecules24112070.

Siveen, K. S., S. Sikka, R. Surana, et al. 2014. "Targeting the STAT3 Signaling Pathway in Cancer: Role of Synthetic and Natural Inhibitors." *Biochimica et Biophysica Acta (BBA) - Reviews on Cancer* 1845, no. 2: 136–154. https://doi.org/10.1016/j.bbcan.2013.12.005.

Tan, H., C. Zhao, Q. Zhu, et al. 2019. "Ursolic Acid Isolated From the Leaves of Loquat (*Eriobotrya japonica*) Inhibited Osteoclast Differentiation Through Targeting Exportin 5." *Journal of Agricultural and Food Chemistry* 67, no. 12: 3333–3340. https://doi.org/10.1021/acs.jafc.8b06954.

Thanou, A., E. Jupe, M. Purushothaman, T. B. Niewold, and M. E. Munroe. 2021. "Clinical Disease Activity and Flare in SLE: Current Concepts and Novel Biomarkers." *Journal of Autoimmunity* 119: 102615. https://doi.org/10.1016/j.jaut.2021.102615.

Wang, Y., R. Jin, J. Chen, et al. 2021. "Tangeretin Maintains Antioxidant Activity by Reducing CUL3 Mediated NRF2 Ubiquitination." *Food Chemistry* 365: 130470. https://doi.org/10.1016/j.foodchem.2021.130470.

Wang, Y., X. J. Liu, J. B. Chen, J. P. Cao, X. Li, and C. D. Sun. 2022. "Citrus Flavonoids and Their Antioxidant Evaluation." *Critical Reviews in Food Science and Nutrition* 62, no. 14: 3833–3854. https://doi.org/10.1080/10408398.2020.1870035.

Wang, Y., J. Qian, J. Cao, et al. 2017. "Antioxidant Capacity, Anticancer Ability and Flavonoids Composition of 35 Citrus (*Citrus reticulata* Blanco) Varieties." *Molecules* 22, no. 7: 1114. https://doi.org/10.3390/molecules22071114.

Wang, Y., W. Zang, S. Ji, J. Cao, and C. Sun. 2019. "Three Polymethoxyflavones Purified From Ougan (*Citrus reticulata* cv. Suavissima) Inhibited LPS-Induced NO Elevation in the Neuroglia BV-2 Cell Line via the JAK2/STAT3 Pathway." *Nutrients* 11, no. 4: 791. https://doi.org/10.3390/nu11040791.

Witthuhn, B. A., F. W. Quelle, O. Silvennoinen, et al. 1993. "JAK2 Associates With the Erythropoietin Receptor and Is Tyrosine Phosphorylated and Activated Following Stimulation With Erythropoietin." *Cell* 74, no. 2: 227–236. https://doi.org/10.1016/0092-8674(93)90414-l.

Wu, R., L. Zhou, Y. Chen, et al. 2022. "Sesquiterpene Glycoside Isolated From Loquat Leaf Targets Gut Microbiota to Prevent Type 2 Diabetes Mellitus in Db/Db Mice." *Food & Function* 13, no. 3: 1519–1534. https://doi.org/10.1039/d1fo03646g.

Xiao, S., W. Wang, and Y. Liu. 2023. "Research Progress on Extraction and Separation of Active Components From Loquat Leaves." *Separations* 10, no. 2: 126. https://doi.org/10.3390/separations10020126.

Xie, Y., W. Zhao, T. Zhou, G. Fan, and Y. Wu. 2010. "An Efficient Strategy Based on MAE, HPLC-DAD-ESI-MS/MS and 2D-prep-HPLC-DAD for the Rapid Extraction, Separation, Identification and Purification of Five Active Coumarin Components From Radix Angelicae Dahuricae." *Phytochemical Analysis* 21, no. 5: 473–482. https://doi.org/10.1002/pca.1222.

Xu, H., X. Li, and J. Chen. 2014. "Comparison of Phenolic Compound Contents and Antioxidant Capacities of Loquat (*Eriobotrya japonica* Lindl.) Fruits." *Food Science and Biotechnology* 23, no. 6: 2013–2020. https://doi.org/10.1007/s10068-014-0274-2.

Yan, Q.-J., Y.-Y. Chen, M.-X. Wu, et al. 2023. "Phenolics and Terpenoids Profiling in Diverse Loquat Fruit Varieties and Systematic Assessment of Their Mitigation of Alcohol-Induced Oxidative Stress." *Antioxidants* 12, no. 10: 1795. https://doi.org/10.3390/antiox12101795.

Yao, Y., T. Liu, L. Yin, S. Man, S. Ye, and L. Ma. 2021. "Polyphenol-Rich Extract From *Litchi chinensis* Seeds Alleviates Hypertension-Induced Renal Damage in Rats." *Journal of Agricultural and Food Chemistry* 69, no. 7: 2138–2148. https://doi.org/10.1021/acs.jafc.0c07046.

Yin, S., L. Niu, J. Zhang, W. Yang, and Y. Liu. 2024. "Berry Beverages: From Bioactives to Antidiabetes Properties and Beverage Processing Technology." *Food Frontiers* 5, no. 4: 1445–1475. https://doi.org/10.1002/fft2.399.

Zeng, K. W., S. Wang, X. Dong, Y. Jiang, and P. F. Tu. 2014. "Sesquiterpene Dimer (DSF-52) From *Artemisia argyi* Inhibits Microglia-Mediated Neuroinflammation via Suppression of NF-κB, JNK/p38 MAPKs and Jak2/Stat3 Signaling Pathways." *Phytomedicine* 21, no. 3: 298–306. https://doi.org/10.1016/j.phymed.2013.08.016.

Zhang, J., Y. Xu, C. T. Ho, et al. 2022. "Phytochemical Profile of Tibetan Native Fruit 'Medog Lemon' and Its Comparison With Other Cultivated Species in China." *Food Chemistry* 372: 131255. https://doi.org/10.1016/j.foodchem.2021.131255.

Zhang, L., X. Li, B. Ma, et al. 2017. "The Tartary Buckwheat Genome Provides Insights Into Rutin Biosynthesis and Abiotic Stress Tolerance." *Molecular Plant* 10, no. 9: 1224–1237. https://doi.org/10.1016/j.molp.2017.08.013.

Zhang, P., L. Zheng, Y. Duan, et al. 2022. “Gut Microbiota Exaggerates Triclosan-Induced Liver Injury via Gut-Liver Axis.” *Journal of Hazardous Materials* 421: 126707. https://doi.org/10.1016/j.jhazmat.2021.126707.

Zheng, Z., and B. Wang. 2021. “The Gut-Liver Axis in Health and Disease: The Role of Gut Microbiota-Derived Signals in Liver Injury and Regeneration.” *Frontiers in Immunology* 12: 775526. https://doi.org/10.3389/fimmu.2021.775526.

Zhu, C. Q., J. B. Chen, C. N. Zhao, et al. 2023. “Advances in Extraction and Purification of Citrus Flavonoids.” *Food Frontiers* 4, no. 2: 750–781. https://doi.org/10.1002/fft2.236.